

Nanoscale phase change on $\text{Ge}_2\text{Sb}_2\text{Te}_5$ thin films induced by optical near fields with photoassisted scanning tunneling microscope

Cite as: Appl. Phys. Lett. **117**, 211102 (2020); <https://doi.org/10.1063/5.0032573>

Submitted: 09 October 2020 . Accepted: 08 November 2020 . Published Online: 24 November 2020

 Kanta Asakawa,  Dang-il Kim,  Shotaro Yaguchi,  Mikito Tsujii,  Katsumasa Yoshioka,  Keisuke Kaneshima,  Yusuke Arashida,  Shoji Yoshida,  Hidemi Shigekawa,  Masashi Kuwahara,  Ikufumi Katayama, and  Jun Takeda



View Online



Export Citation



CrossMark



Your Qubits. Measured.

Meet the next generation of quantum analyzers

- Readout for up to 64 qubits
- Operation at up to 8.5 GHz, mixer-calibration-free
- Signal optimization with minimal latency

Find out more



Nanoscale phase change on $\text{Ge}_2\text{Sb}_2\text{Te}_5$ thin films induced by optical near fields with photoassisted scanning tunneling microscope

Cite as: Appl. Phys. Lett. **117**, 211102 (2020); doi: [10.1063/5.0032573](https://doi.org/10.1063/5.0032573)

Submitted: 9 October 2020 · Accepted: 8 November 2020 ·

Published Online: 24 November 2020



View Online



Export Citation



CrossMark

Kanta Asakawa,^{1,2,a)}  Dang-il Kim,¹ Shotaro Yaguchi,¹ Mikito Tsujii,¹ Katsumasa Yoshioka,¹ 
Keisuke Kaneshima,¹  Yusuke Arashida,^{1,3} Shoji Yoshida,³ Hidemi Shigekawa,³ Masashi Kuwahara,⁴ 
Ikufumi Katayama,¹  and Jun Takeda^{1,a)} 

AFFILIATIONS

¹Department of Physics, Graduate School of Engineering Science, Yokohama National University, Yokohama 240-8501, Japan

²Department of Applied Physics, Tokyo University of Agriculture and Technology, Koganei, Tokyo 184-8588, Japan

³Faculty of Pure and Applied Sciences, University of Tsukuba, Tsukuba 305-8571, Japan

⁴Sensing System Research Center, National Institute of Advanced Industrial Science and Technology, Central 5, 1-1-1 Higashi, Tsukuba, Ibaraki 305-8562, Japan

^{a)}Authors to whom correspondence should be addressed: jun@ynu.ac.jp and asakawa@go.tuat.ac.jp

ABSTRACT

A scanning probe microscope coupled with either femtosecond laser pulses or terahertz pulses holds great promise not only for observing ultrafast phenomena but also for fabricating desirable structures at the nanoscale. In this study, we demonstrate that a few-nanometer-scale phase change can be non-thermally stored on the $\text{Ge}_2\text{Sb}_2\text{Te}_5$ surface by a laser-driven scanning tunneling microscope (STM). An atomically flat $\text{Ge}_2\text{Sb}_2\text{Te}_5$ surface was irradiated with the optical near-field generated by introducing femtosecond laser pulses to the STM tip-sample junction. The STM topographic images showed that few-nanometer-scale mounds appeared after irradiation. In addition, tunneling conductance spectra showed that the bandgap increased by 0.2 eV in the area of $5 \times 5 \text{ nm}^2$. These indicate that the nanoscale crystal-to-amorphous phase change was induced by the STM-tip-induced near field. Our approach presented here offers an unprecedented increase in the recording density of optical storage devices and is, therefore, expected to facilitate the development of next-generation information technology.

Published under license by AIP Publishing. <https://doi.org/10.1063/5.0032573>

In optical storage devices such as DVD-RAM, information is recorded on phase change materials (PCMs) of which structural phases can be optically switched and detected.¹⁻³ PCMs have recently attracted much attention as candidate materials for phase change random access memory (PCRAM),^{4,5} which is a next generation nonvolatile electrical memory that utilizes the resistance contrast. Among PCMs, $\text{Ge}_2\text{Sb}_2\text{Te}_5$ (GST) is a representative example: it has two crystalline phases, the metastable face-centered cubic (fcc) and the stable hexagonal close-packed (hcp) phases, and an amorphous phase.^{6,7} The fcc phase can be thermally transformed into the amorphous phase via the liquid phase by laser irradiation. The amorphized region can be conversely crystallized in the fcc structure by weak heating. This enables us to repeatedly write and erase the information.

The recording capacity of optical storage is determined by the size and the positional uncertainty of the amorphous/crystal-phase spots, which are in general limited by the diffraction limit of light. So

far, many attempts have been examined to reduce the spot size. By heating a small area of the GST surface with gold antennas in a $5 \mu\text{m}$ gap, the size of amorphous marks can be reduced below the diffraction limit.⁸ Sato *et al.* demonstrated that nanoscale amorphous marks can be created by applying voltage pulses from the tip of a scanning probe microscope (SPM).^{9,10} However, the heat generated in small areas often damages the sample and its structural configuration, and the smallest mark size is still limited to $\sim 10 \text{ nm}$, which can be explained using a thermodynamic model. In addition, the recording speed of conventional optical storage devices and PCRAMs is limited by thermal processes including melting, quenching, and crystallization.¹¹ To overcome these problems, a technique should be developed to non-thermally induce the phase change in small areas.

It has been reported that GST can be amorphized non-thermally by femtosecond laser irradiation.¹²⁻¹⁴ The mechanism of the non-thermal amorphization is explained by the flipping of the Ge atom

from the octahedral symmetry site to the tetrahedral symmetry site assisted by the optical excitation of electrons in the valence band to the conduction band.^{15,16} The non-thermal ultrafast amorphization of GST has been achieved with various center wavelengths ranging from 800 to 1500 nm^{12–14,17} presumably because the optical excitation of valence band electrons only requires the photon energy larger than the bandgap. Implementation of this non-thermal ultrafast amorphization with an ultrashort pulsed laser is expected to minimize the heating effect, which is critical for realizing high-density and high-speed recording.

Recently, SPMs combined with either ultrashort laser pulses or terahertz pulses have been extensively developed to image electronic properties of materials with high spatiotemporal resolutions.^{18–21} These techniques allow us not only to track the motion of single molecules but also to coherently control the motion of electrons.^{22–24} The tip-enhanced electric near field produced by irradiating the tip-sample junction with laser pulses is strongly confined and can be utilized to fabricate nanoscale structures.^{25–29} In this study, we demonstrate the utilization of the optical near field generated by irradiating a scanning tunneling microscope (STM) tip with femtosecond laser pulses for creating nanoscale amorphous marks, which will contribute to realizing the high-density recording technique.

Figure 1 shows a schematic of the experimental apparatus. The STM and scanning tunneling spectroscopy (STS) experiments were conducted at room temperature with an ultra-high vacuum (UHV) STM system with a base pressure lower than 1×10^{-7} Pa. A mechanically sharpened PtIr wire was used as a probing tip. Laser pulses with the incidence angle with respect to the sample surface of 45° , the center wavelength of 1035 nm, and the pulse duration of 300 fs generated by a fiber laser amplifier were focused to the tip-sample junction by a lens in the STM measurement chamber. The repetition rate and the fluence of each pulse were 100 kHz and $107\text{--}127$ mJ/cm², respectively. We carefully confirmed that the fluence was enough to induce the crystal-to-amorphous phase change on GST without ablation. The beam waist diameter of the incident laser pulses was designed to be $10\ \mu\text{m}$, which was verified using a charge-coupled device (CCD)

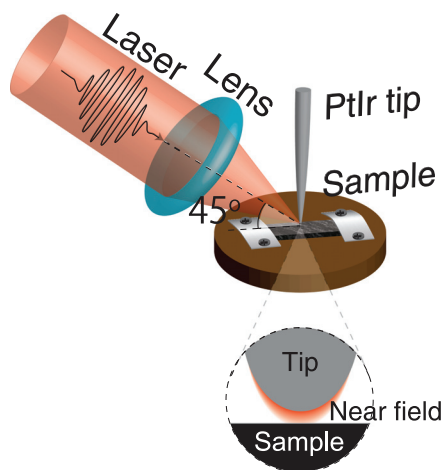


FIG. 1. Schematic of the photoassisted STM. When the laser pulses were applied to a tip-sample junction, the tip was lifted by 5 nm far from the sample before the laser irradiation, to avoid tip crash due to thermal expansion of the tip.

camera. The tip was retracted by 5 nm from the surface during laser irradiation to avoid tip crash due to the thermal expansion of the tip. Since the amorphization induced by a single-laser-pulse irradiation occurred with much less efficiency, we implemented the irradiation of 2000–10 000 laser pulses with a time interval of $10\ \mu\text{s}$, which ensured high producibility of the photoassisted amorphization. The relatively long time interval also may minimize the thermal process for the photoassisted amorphization.

GST thin films with a 100–300 nm thickness, which is thick enough to prevent ablation,¹⁴ were sputter-deposited onto a cleaved highly oriented pyrolytic graphite (HOPG) surface at room temperature. The deposition rate was set to 0.714 nm/s. After taking out from the deposition chamber into air, the samples were dipped in distilled water for one minute to remove the oxidized layer.^{30,31} After loading the samples into the STM chamber, the samples were annealed in UHV for crystallization and to flatten the surfaces atomically.³² Notably, to obtain the fcc phase, the temperature should not exceed 300°C during the whole procedure as GST transforms into the hcp phase at 310°C .

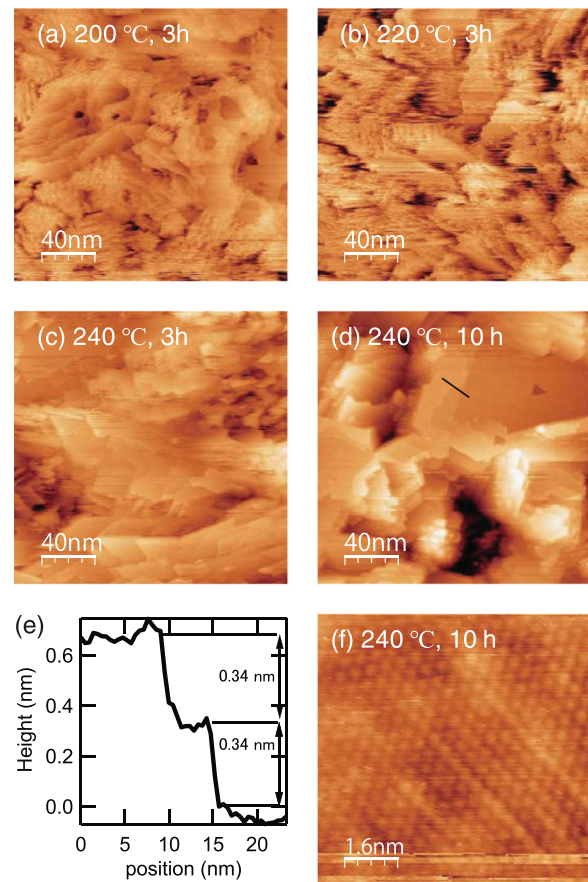


FIG. 2. STM images of $\text{Ge}_2\text{Sb}_2\text{Te}_5(300\text{nm})/\text{HOPG}$ surfaces prepared by dipping them in distilled water and UHV annealing at (a) 200°C for 3 h, (b) at 220°C for 3 h, (c) at 240°C for 3 h, and (d) at 240°C for 10 h. (e) The line profile of (d) whose position is indicated by the black line. (f) The atomic image of the sample obtained by the same preparation procedure as (d) taken with $V_s = -50$ mV and $I_t = 20$ pA.

Figures 2(a)–2(c) show the STM images of the samples annealed for 3 h at 200, 220, and 240 °C, respectively, recorded with the sample bias voltage (V_s) of 5 V and the tunneling current (I_t) of 5 pA. The sample annealed at 240 °C had a clear step-terrace structure, whereas the structures of samples annealed at 200 and 220 °C were unclear. The areas of the terraces were enlarged by increasing the annealing time to 10 h, as shown in Fig. 2(d). The step height was estimated as 0.34 nm from the line profile as shown in Fig. 2(e), which agreed well with the distance between neighboring Te layers^{30,33} and is significantly different from the interlayer distance of the hcp phase.^{16,34} The atomic image shown in Fig. 2(f) exhibits a defect-free hexagonal array with a distance between atoms of 0.41 ± 0.01 nm, which indicates that the surface is the Te-terminated GST (111) surface.³⁰ Based on these results, the GST film prepared by annealing at 240 °C for 10 h was appraised as having a crystalline phase with a fcc structure.

Figures 3(a) and 3(b) show the STM images taken before and after the irradiation, respectively, and Fig. 3(c) shows the line profiles of the location indicated by the black bars. Atomic corrugations are faintly visible in Figs. 3(a) and 3(b) and their periodicity is consistent with that of Te-terminated GST (111) surfaces, which was confirmed by two-dimensional fast Fourier transformation. A mound-like feature with a height of ≈ 0.3 nm and a width of ≈ 4 nm was formed by laser irradiation. All the scan lines within ~ 2 nanometers from the irradiation point exhibited a similar feature, which indicates that a nanoscale mound was formed by laser irradiation. Figure 3(d) shows the tunneling current–voltage (I – V) curves and differential tunneling conductance (dI/dV) spectra measured at the location shown by the black dots in (a) and (b). The difference in the position is due to the thermal drift. The dI/dV spectra were obtained by numerically differentiating the I – V curve measured after stabilizing the tip height at $V_s = -100$ mV and $I_t = 20$ pA. The differential conductance spectrum before laser irradiation exhibits a bandgap, and the Fermi level is

located near the top of the valence band, which indicates that the sample is a p-type semiconductor. The p-type carriers are typically attributed to excess vacancies.^{35–38} The few-atom-scale contrast in atomic images can also be attributed to the spatial distribution of the density of excess vacancies. The conduction band bottom moved upward by ≈ 0.2 eV after laser irradiation, indicating that the region was amorphized by a tip-enhanced near field.³⁹ The formation of a mound can also be explained by the lattice expansion of GST by amorphization.³³ From the observed height of the amorphous mound and the expansion rate of 4.6%,³³ the depth of the amorphous region is roughly estimated to be 7 nm. The defect-free atomic rows are still faintly visible after amorphization, suggesting that the amorphization is driven non-thermally without liquidization.^{16,40}

The height of the amorphous mound is lower than the surface roughness, which means that it is difficult to detect the amorphized region only from the topographic image. On the other hand, the shapes of I – V curves, which reflect the local density of states (DOS) of electrons, are not disturbed by the surface morphology. The I – V curve is, thereby, more suitable for detection of the amorphous region, and the tunneling current mapping before and after laser irradiation was implemented. As only the conduction band bottom moves upward by amorphization³⁹ [see Fig. 3(d)], the rising edge in the positive bias region of the I – V curves shifts upward, leading to the decrease in current at the positive bias. Figure 4(a) shows a 100 nm \times 100 nm topographic image of the GST(100 nm)/HOPG surface. The root mean square roughness was 2.69 nm, which is one order of magnitude larger than the height of the mound (≈ 0.3 nm) formed by amorphization. The laser pulses were introduced after settling the tip at the position represented by the green dot. We measured I – V curves after stabilizing the tip-sample distance at $V_s = -600$ mV and $I_t = 70$ pA at the centers of each square in the grid pattern with 5 nm intervals arranged in the area of Fig. 4(a) before and after the irradiation. The I – V curves before irradiation show p-type semiconducting behavior. After the irradiation, bandgap broadening was observed only at the irradiated point. These results well reproduced the result shown in Fig. 3(d). Here, we introduce the normalized tunneling current $-I(V = -200 \text{ mV})/I(V = 600 \text{ mV})$ for the evaluation of the area of the laser-induced amorphization. Based on this treatment, we could minimize the deterioration of the signal-to-noise ratio caused by the instability of tip-sample distance.⁴¹ Figures 4(b) and 4(c) show the $-I(V = -200 \text{ mV})/I(V = 600 \text{ mV})$ mappings before and after the irradiation, respectively. The small shift of the green dot indicating the irradiated position is due to the thermal drift. A bright protrusion corresponding to the laser-induced amorphous region clearly appears at the spot, whose intensity (13.1) is much larger than the standard deviation (0.34) of the background region. This demonstrates that the amorphous area could be sensitively detected with a good signal-to-noise ratio by utilizing the I – V characteristics, even if the topographic image is not flat enough to resolve the height of the amorphous mound. We also found that the size of the laser-induced amorphous region was comparable to the pixel size (5 nm \times 5 nm), which is significantly smaller than the smallest thermally created amorphous marks.⁹ This indicates that a nanoscale crystal-to-amorphous phase change was induced non-thermally by the STM-tip-induced near field and that the tip-enhanced near field is localized within few-nanometer area, which is smaller than the typical tip apex radius (10–100 nm). This is supported by simulation results showing that the near field is

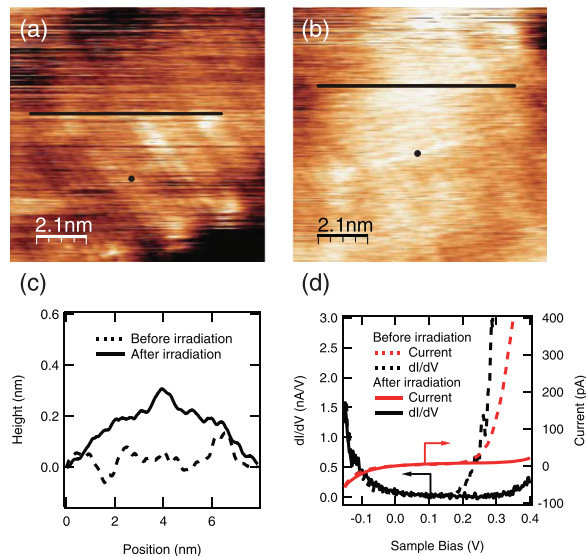


FIG. 3. STM images taken (a) before and (b) after laser irradiation. (c) The line profiles of the location indicated by black bars in (a) and (b). (d) I – V curve and differential tunneling conductance spectra measured at the location indicated by black dots in (a) and (b).

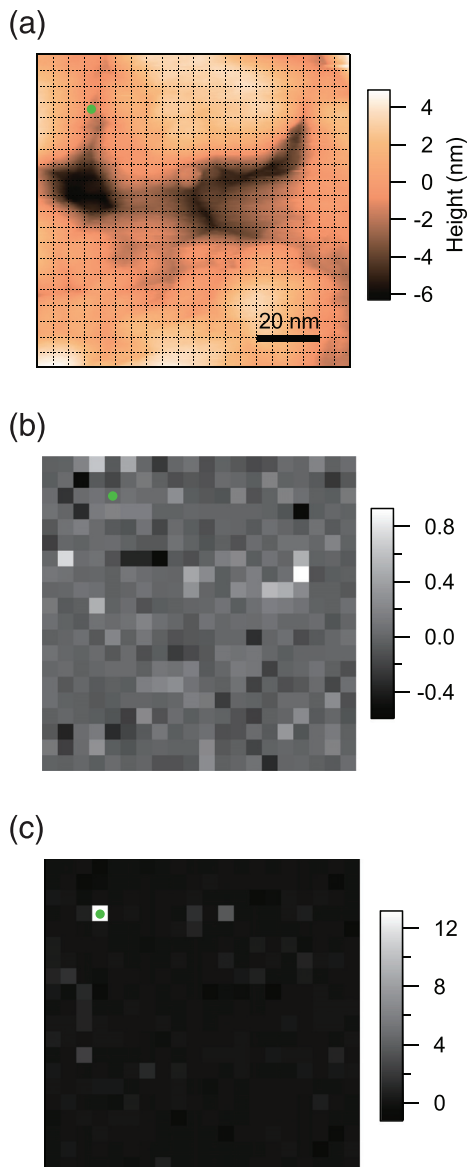


FIG. 4. (a) Topographic image of $\text{Ge}_2\text{Sb}_2\text{Te}_5(100 \text{ nm})/\text{HOPG}$ surface with a $100 \text{ nm} \times 100 \text{ nm}$ area. (b) $-I(V = -200 \text{ mV})/I(V = 600 \text{ mV})$ mapping of the same area as (a) before and (c) after laser irradiation.

localized within a few nanometers from the tip center due to the field enhancement by the tip-sample gap.^{29,42} It is well known that the amorphous-to-crystalline phase change can be introduced by either weak heating^{6,7} or irradiating with intense terahertz pulses.⁸ These will be conducted in the future to examine the rewritable characteristics of the nanoscale phase change of GST.

In conclusion, we have demonstrated that STM coupled with femtosecond laser pulses can be utilized to non-thermally create nanometer-scale amorphous marks on GST surfaces. The amorphous region can be detected through either the changes in the topographic

images or the change in the I - V characteristics originating from the bandgap broadening. Because both generation of optical near fields by SPM tips and the non-thermal amorphization of GST can support a wide range of wavelengths,^{12-14,17} our concept presented here should work with various laser sources and may help in increasing the information storage density of memory devices.

This work was supported in part by the Grants-in-Aid for Scientific Research (KAKENHI Nos. 17H06124, 17H06088, 18H04288, 20H00326, and 20H05662 from the Japan Society for the Promotion of Science (JSPS). The STM topographic images were processed using WSxM.⁴³

DATA AVAILABILITY

The data that support the findings of this study are available from the corresponding author upon reasonable request.

REFERENCES

- ¹R. Von Gutfeld and P. Chaudhari, *J. Appl. Phys.* **43**, 4688 (1972).
- ²V. Weidenhof, I. Friedrich, S. Ziegler, and M. Wuttig, *J. Appl. Phys.* **89**, 3168 (2001).
- ³T. Matsunaga, J. Akola, S. Kohara, T. Honma, K. Kobayashi, E. Ikenaga, R. O. Jones, N. Yamada, M. Takata, and R. Kojima, *Nat. Mater.* **10**, 129 (2011).
- ⁴S. Raoux, G. W. Burr, M. J. Breitwisch, C. T. Rettner, Y.-C. Chen, R. M. Shelby, M. Salinga, D. Krebs, S.-H. Chen, H.-L. Lung *et al.*, *IBM J. Res. Dev.* **52**, 465 (2008).
- ⁵F. Rao, K. Ding, Y. Zhou, Y. Zheng, M. Xia, S. Lv, Z. Song, S. Feng, I. Ronneberger, R. Mazzarello *et al.*, *Science* **358**, 1423 (2017).
- ⁶N. Yamada, E. Ohno, K. Nishiuchi, N. Akahira, and M. Takao, *J. Appl. Phys.* **69**, 2849 (1991).
- ⁷I. Friedrich, V. Weidenhof, W. Njoroge, P. Franz, and M. Wuttig, *J. Appl. Phys.* **87**, 4130 (2000).
- ⁸Y. Sanari, T. Tachizaki, Y. Saito, K. Makino, P. Fons, A. V. Kolobov, J. Tominaga, K. Tanaka, Y. Kanemitsu, M. Hase *et al.*, *Phys. Rev. Lett.* **121**, 165702 (2018).
- ⁹H. Satoh, K. Sugawara, and K. Tanaka, *J. Appl. Phys.* **99**, 024306 (2006).
- ¹⁰K. Tanaka, T. Gotoh, and K. Sugawara, *J. Optoelectron. Adv. Mater.* **6**, 1133 (2004).
- ¹¹M. Wuttig and N. Yamada, *Nat. Mater.* **6**, 824 (2007).
- ¹²M. Hada, W. Oba, M. Kuwahara, I. Katayama, T. Saiki, J. Takeda, and K. G. Nakamura, *Sci. Rep.* **5**, 13530 (2015).
- ¹³M. Konishi, H. Santo, Y. Hongo, K. Tajima, M. Hosoi, and T. Saiki, *Appl. Opt.* **49**, 3470 (2010).
- ¹⁴S. H. Møller, E. H. Eriksen, P. L. Tønning, P. B. Jensen, J. Chevallier, and P. Balling, *Appl. Surf. Sci.* **476**, 221 (2019).
- ¹⁵X.-B. Li, X. Liu, X. Liu, D. Han, Z. Zhang, X. Han, H.-B. Sun, and S. Zhang, *Phys. Rev. Lett.* **107**, 015501 (2011).
- ¹⁶A. V. Kolobov, P. Fons, A. I. Frenkel, A. L. Ankudinov, J. Tominaga, and T. Uruga, *Nat. Mater.* **3**, 703 (2004).
- ¹⁷J. Takeda, W. Oba, Y. Minami, T. Saiki, and I. Katayama, *Appl. Phys. Lett.* **104**, 261903 (2014).
- ¹⁸P. Klarskov, H. Kim, V. L. Colvin, and D. M. Mittleman, *ACS Photonics* **4**, 2676 (2017).
- ¹⁹T. L. Cocker, V. Jelic, M. Gupta, S. J. Molesky, J. A. Burgess, G. De Los Reyes, L. V. Titova, Y. Y. Tsui, M. R. Freeman, and F. A. Hegmann, *Nat. Photonics* **7**, 620 (2013).
- ²⁰V. Jelic, K. Iwaszczuk, P. H. Nguyen, C. Rathje, G. J. Hornig, H. M. Sharum, J. R. Hoffman, M. R. Freeman, and F. A. Hegmann, *Nat. Phys.* **13**, 591 (2017).
- ²¹Y. Terada, S. Yoshida, O. Takeuchi, and H. Shigekawa, *Nat. Photonics* **4**, 869 (2010).
- ²²T. L. Cocker, D. Peller, P. Yu, J. Repp, and R. Huber, *Nature* **539**, 263 (2016).
- ²³K. Yoshioka, I. Katayama, Y. Minami, M. Kitajima, S. Yoshida, H. Shigekawa, and J. Takeda, *Nat. Photonics* **10**, 762 (2016).

- ²⁴K. Yoshioka, I. Katayama, Y. Arashida, A. Ban, Y. Kawada, K. Konishi, H. Takahashi, and J. Takeda, *Nano Lett.* **18**, 5198 (2018).
- ²⁵S. Huang, M. Hong, Y. Lu, B. Lukyanchuk, W. Song, and T. Chong, *J. Appl. Phys.* **91**, 3268 (2002).
- ²⁶A. Chimmalgi, D. J. Hwang, and C. P. Grigoropoulos, *Nano Lett.* **5**, 1924 (2005).
- ²⁷A. Chimmalgi, C. Grigoropoulos, and K. Komvopoulos, *J. Appl. Phys.* **97**, 104319 (2005).
- ²⁸A. Chimmalgi, T. Choi, C. Grigoropoulos, and K. Komvopoulos, *Appl. Phys. Lett.* **82**, 1146 (2003).
- ²⁹Y. Chen, Y. Xu, D. Xie, J. Jiang, and Y. Yue, *Appl. Therm. Eng.* **148**, 129 (2019).
- ³⁰C. Pauly, M. Liebmann, A. Giussani, J. Kellner, S. Just, J. Sánchez-Barriga, E. Rienks, O. Rader, R. Calarco, G. Bihlmayer *et al.*, *Appl. Phys. Lett.* **103**, 243109 (2013).
- ³¹Z. Zhang, J. Pan, Y. L. Foo, L. W.-W. Fang, Y.-C. Yeo, R. Zhao, L. Shi, and T.-C. Chong, *Appl. Surf. Sci.* **256**, 7696 (2010).
- ³²H. Dieker and M. Wuttig, *Thin Solid Films* **478**, 248 (2005).
- ³³T. Nonaka, G. Ohbayashi, Y. Toriumi, Y. Mori, and H. Hashimoto, *Thin Solid Films* **370**, 258 (2000).
- ³⁴Y. Pan, Z. Li, and Z. Guo, *Crystals* **9**, 136 (2019).
- ³⁵J. Kellner, G. Bihlmayer, V. Deringer, M. Liebmann, C. Pauly, A. Giussani, J. Boschker, R. Calarco, R. Dronskowski, and M. Morgenstern, *Phys. Rev. B* **96**, 245408 (2017).
- ³⁶M. Wuttig, D. Lüsebrink, D. Wamwangi, W. Welnic, M. Gilleßen, and R. Dronskowski, *Nat. Mater.* **6**, 122 (2007).
- ³⁷A. H. Edwards, A. C. Pineda, P. A. Schultz, M. G. Martin, A. P. Thompson, H. P. Hjalmarson, and C. J. Umrigar, *Phys. Rev. B* **73**, 045210 (2006).
- ³⁸T. Schafer, P. M. Konze, J. D. Huyeng, V. L. Deringer, T. Lesieur, P. Muller, M. Morgenstern, R. Dronskowski, and M. Wuttig, *Chem. Mater.* **29**, 6749 (2017).
- ³⁹T. Kato and K. Tanaka, *Jpn. J. Appl. Phys., Part 1* **44**, 7340 (2005).
- ⁴⁰K. Makino, J. Tominaga, and M. Hase, *Opt. Express* **19**, 1260 (2011).
- ⁴¹A. Stępniański, M. Caminale, A. Leon Vanegas, H. Oka, D. Sander, and J. Kirschner, *AIP Adv.* **5**, 017125 (2015).
- ⁴²X. Shi, N. Coca-López, J. Janik, and A. Hartschuh, *Chem. Rev.* **117**, 4945 (2017).
- ⁴³I. Horcas, R. Fernández, J. Gomez-Rodriguez, J. Colchero, J. Gómez-Herrero, and A. Baro, *Rev. Sci. Instrum.* **78**, 013705 (2007).